

CHAPTER 5

ESTIMATION OF PRECIPITATION BY RADAR

5.1 Introduction. The accurate measurement of precipitation plays a very important role in hydrology, agriculture, weather modification, climatology, and weather forecasting. The primary requirement of radar for hydrological purposes is to provide estimates of the amount and the temporal and spatial distribution of precipitation that falls over a watershed. For many agricultural applications and climatic studies, precipitation data are needed over large areas for long periods (days or weeks) and a relatively sparse network of rain gages reporting once per day may be adequate. In contrast, measurements from many closely spaced stations are required to forecast flash floods on streams, where data are required for short time intervals (<6 hours) and over small areas [$<1000 \text{ km}^2$ ($<290 \text{ nm}^2$)]. Also, to evaluate weather modification experiments, high-resolution spatial and temporal data are needed. However, it is generally not practical to install and to maintain a sufficient number of closely spaced in situ observation sites that transmit timely data to a central processing facility. Hence, weather radar precipitation estimates provide a practical data source not available by other means. Development of procedures for using radar as a tool to measure precipitation has progressed from the subjective manual techniques, first used in the late 1940s, through the semi-automatic techniques, to the fully automatic techniques of today.

Radar does not measure precipitation rate directly, but rather estimates that rate from the backscattered energy received from precipitation particles in an elevated volume. Consequently, radar estimates of precipitation, due to the variability in the relationship between the backscattered energy and precipitation rate, are subject to sampling and measurement errors. Other errors also potentially come into play when estimating precipitation by radar as well as by the combination of radar and rain gages. These will be discussed in subsequent sections of this chapter.

5.2 Physical Principles of the Measurement Process. A more detailed description of the physics pertaining to the measurement process is provided in Appendix A. The following discussion highlights the relationship between the meteorological quantities of particle size distribution, radar reflectivity factor, and precipitation rate.

5.2.1 Particle Size Distributions. Except for small diameters ($D < 1 \text{ mm}$), particle size distributions for rain and snow can be approximated by:

$$N(D) = N_0 e^{-\Lambda D} \quad (5-1)$$

where $N(D)$ is the number concentration of size D droplets per volume interval, Λ is the mean drop size, and N_0 is the number of particles per unit volume (Marshall and Palmer 1948). For a snow particle, D is the diameter of a droplet of equal mass. From raindrop records collected on

dyed filter paper for an entire summer, Marshall and Palmer determined N_0 to be $8000 \text{ m}^{-3} \text{ mm}^{-1}$ and Λ to be $4.1R^{-2.1} \text{ mm}^{-1}$, where R is the rainfall rate (mm h^{-1}). Of course, there are significant departures from these parametric values for other precipitation regimes and, in fact, the relationship may differ markedly from a simple exponential relationship with individual drop size samples and with certain types of precipitation. Numerous other investigations have reemphasized that Λ and N can vary from storm to storm and that N_0 is also a function of precipitation rate. In general, both parameters, N_0 and Λ , are needed to specify the size distribution.

5.2.2 Radar Reflectivity Factor. When the drop size distribution is known, radar reflectivity factor, Z , in a unit volume can be calculated from:

$$Z = \int_0^{\infty} D^6 N(D) dD \quad (5-2)$$

Alternatively, Z can be estimated using the radar equation:

$$Z = \frac{2^{10} (\ln 2)}{\pi^3 c} \left[\frac{\lambda^2}{P_t \tau G^2 \theta_{3dB}^2} \right] \left[\frac{r^2 \bar{P}_r}{|K|^2} \right] \quad (5-3)$$

where:

- P_r = average return power, watts
- P_t = peak transmitted power, watts
- G = antenna gain, dimensionless
- λ = radar wavelength, meter
- θ_{3dB} = antenna half-power beam width, radian
- τ = pulse duration, second
- c = electromagnetic propagation constant (speed of light) = $3(10^8) \text{ m s}^{-1}$
- r = range to target, meter
- K = complex index of refraction; $|K|^2$ is conventionally taken to be 0.93 for water and 0.2 for ice
- Z = radar reflectivity factor

This equation assumes that:

- The particles are small, homogeneous spheres conforming to Rayleigh scattering principles;
- The particles are spread uniformly throughout the contributing region;
- The reflectivity factor, Z , is uniform throughout the contributing region and constant over the sampling interval;
- All particles have the same dielectric constant, $|K|^2$, i.e., it is not mixed precipitation;
- The main lobe of the antenna beam pattern is described adequately by a Gaussian function;
- Microwave attenuation and multiple scattering are negligible; and
- Incident and back-scattered waves are linearly polarized.

If all assumptions were able to be met and if no measurement errors existed, the radar measured Z (Eq. 5-3) would conform to the meteorologically defined Z (Eq. 5-2). However, this is not the case and it is, therefore, customary to use Z_e , the equivalent radar reflectivity factor, in the radar equation as shown in Appendix A, which can be simplified as:

$$\bar{P}_r = \frac{C Z_e}{r^2} \quad (5-4)$$

where C is a combination of all known constants in the equation. Z_e can be calculated if \bar{P}_r and r are known.

In the same way that Z can be related to drop size distribution, the precipitation rate, R , when the vertical airspeed is zero, as it is at the ground, can be given by:

$$R = \frac{\pi}{6} \int_0^{\infty} D^3 v_t (D) N(D) dD \quad (5-5)$$

Attempts have been made to combine Eqs. (5-2) and (5-5) in order to obtain an analytical relationship between Z and R , but a number of problems are encountered. First, spatial and temporal variations of particle size distributions are rarely known and, second, vertical air motions are frequently of the same magnitude as the particle terminal fall speeds (particularly in

thunderstorms). Finally, different drop size distributions can result in the same Z yielding different values of R.

5.2.3 Reflectivity-Precipitation Relationship. A unique relationship between Z and R does not actually exist. But if all the assumptions introduced to develop Eqs. (5-2) and (5-5) hold true and one assumes that N_0 is constant, then a single parameter relationship $R = R(Z)$ is implied. This relationship is generally expressed in the form:

$$Z = AR^b \quad (5-6)$$

There has been much empirical study to identify values of the coefficient (A) and exponent (b) in Eq. (5-6). The parameters for rainfall reported by different investigations range from less than 20 to more than 1000 for the coefficient and from 1.11 to 3.05 for the exponent. In most cases, as the Z-R's coefficient increases the exponent decreases.

5.3 Error Sources in Radar Measurements. The factors causing errors in the radar measurement of surface precipitation can be grouped into four broad categories: 1) estimating equivalent radar reflectivity factor, 2) variations in the Z-R relationship, 3) time and space averaging of precipitation measurement by radar, and 4) below-beam effects. These categories are described in the following sections.

5.3.1 Estimating Equivalent Radar Reflectivity Factor. The equivalent radar reflectivity factor may be biased by a number of factors such as incorrect hardware calibration, ground clutter, anomalous propagation, partial beam filling, and wet radome attenuation.

System errors (bias) in the measurement of reflectivity arise from incorrect hardware calibration. Even after careful electronic system calibration, large, inexplicable errors in precipitation estimates occasionally remain. Usually, losses are greater than estimated and precipitation amounts are underestimated accordingly, although the opposite effect is also possible.

A potentially serious source of error, not associated with hardware, is blockage by ground targets close to the radar site such as trees, buildings, and ridges that can severely reduce the effective transmitted and received power and cause recurring shadows in precipitation patterns. Correction for blockage can be performed by addition of an adjustment factor or interpolation with neighboring bins as described in Part C, Chapter 3, of this Handbook.

Vertical gradients in atmospheric temperature, humidity, and pressure cause a gradient in the refractive index. This causes the radar beam to be bent in a characteristic manner for standard atmospheric conditions. Non-standard atmospheric conditions, and the associated non-standard gradient in the refractive index, can result in AP (Part D, Section 4.2.1 and Part B, Section 3.4.2 of this Handbook) of the radar beam and can produce significant errors in reflectivity estimates. Temperature inversions, with decreasing moisture with height, cause bending or even ducting of

radar signals, resulting in ground target returns from extended ranges. This condition is sometimes widespread; a local condition, dubbed thunderstorm super-refraction, occurs when local temperature inversions and specific humidity fluctuations are produced by downdrafts spreading beneath thunderstorms. In regions of super-refraction and their attendant shadow zones, precipitation estimates may be significantly reduced. AP can often be identified by a large variance of spatial reflectivity and by a small rate of echo fluctuations.

Ground clutter and AP are most likely to corrupt reflectivity estimates from radar signals at lower elevations. As a result, these effects can be reduced by an appropriate selection of reflectivity data from four sequentially obtained contiguous low elevation scans (Fulton et al. 1998). Development of the "hybrid scan" is described in Part C, Chapter 3, of this Handbook.

Signal degradation, partial beam filling, and radar horizon reduce precipitation rate estimates at longer ranges (Wilson 1975; Hudlow et al. 1979). This is known as the range effect. The range effect has been found to be correlated with echo intensity (or precipitation rate) and is greater in shallow precipitation regimes. The hybrid scan significantly reduces the range effect, but an additional range-dependent, site-varying correction is also applied to the precipitation rate data (Ahnert et al. 1983). (An exception to the range effect is seen with convective storms which normally are characterized by an elevated reflectivity maximum. The radar horizon will then lead to rainfall overestimation in convective storm situations at longer ranges.)

When the radome that encloses the radar antenna is wet, attenuation of the radar signal increases. This increased attenuation is a function of water film thickness and radar wavelength and may approach 1 dB for the WSR-88D. Because this temporary condition is difficult to describe quantitatively and because recovery is rapid once precipitation has ended, usually no attempt is made to account for this loss for S-band radars. Since wet radome attenuation introduces systematic bias, adjustment with rain gage data helps via the adjustment algorithm and the external bias factor generated externally to the radar system.

5.3.2 Variations in the Z-R Relationship. Many studies of the relationship between Z and R have been made, especially for rain. If the particle size distribution were a unique function of the precipitation rate, a universal Z-R relationship for rain would exist. However, it has been amply demonstrated that there is no unique particle size distribution for a given precipitation rate or even for a given storm. The literature on the subject of Z-R relationships for rain is too extensive to be reviewed in detail in this section; however some of the more significant results are discussed below.

One of the earliest and most familiar relations is:

$$Z = 200R^{1.6} \tag{5-7}$$

following the work of Marshall and Palmer (1948).

Numerous measurements of drop size distributions have been made in stratiform rain, rain showers, and thunderstorms; and the characteristic Z-R relationships are reported in the literature (e.g., Battan 1973). Ordinarily the coefficient in Eq. (5-6) increases as the precipitation becomes more convective. For example, Joss et al. (1970) gave:

$$\text{Drizzle} \quad Z = 140R^{1.5} \quad (5-8)$$

$$\text{Thunderstorms} \quad Z = 500R^{1.5} \quad (5-9).$$

The presence of larger raindrops in thunderstorms causes the coefficient to be larger.

Drop size measurements beneath a large Oklahoma thunderstorm (Martner 1977) yielded these relationships:

$$\text{Leading portion} \quad Z = 667R^{1.33} \quad (5-10)$$

$$\text{Central core} \quad Z = 124R^{1.64} \quad (5-11)$$

$$\text{Trailing portion} \quad Z = 436R^{1.43} \quad (5-12).$$

A mean Z-R relationship for snow, where R is an equivalent rain rate, is:

$$Z = 2000R^2 \quad (5-13).$$

Hail Z-R relationships depend upon the stone density, i.e., whether growth has been dry or wet, and the thickness of water films. Douglas (1963) found:

$$\text{Wet growth} \quad Z = 84000R^{1.29} \quad (5-14)$$

$$\text{Dry growth} \quad Z = 22500R^{1.17} \quad (5-15).$$

Considering all of the above, the coefficient and exponent in the Z-R relationship used with the WSR-88D hydrologic software are adaptable parameters with default values set at:

$$Z = 300R^{1.4} \quad (5-16)$$

or for tropical convective systems, particularly during land falling hurricanes and tropical storms (Rosenfeld et al. 1993)

$$Z = 250R^{1.2} \quad (5-17).$$

Based on several years of WSR-88D experience and studies of cool season stratiform rain events (Super and Holroyd 1998; Carins et al. 1998; Huggins and Kingsmill 1998; and Quinlan and

Sinsabaugh 1999) have shown that the best Z-R relationship depends significantly on geographic location. The ROC recommends the following Z-R relationships:

Winter stratiform precipitation (east of Continental Divide) and orographic rain (East)

$$Z = 130R^{2.0} \quad (5-18)$$

Winter stratiform precipitation (west of Continental Divide) and orographic rain (West)

$$Z = 75R^{2.0} \quad (5-19)$$

Figure 5-1 gives examples of Z-R relationships for various forms of precipitation. As can be seen in Figure 5-1, use of Eq. (5-16) with the WSR-88D hydrologic software should provide a good average for different precipitation types.

Though the multiplicative coefficient chosen for Eq. (5-16) strongly affects the accuracy of the estimates, this coefficient can be adjusted using coincident rain gauge observations (Seo et al. 1999). This was done in establishing the default tropical relationship of Eq. (5-17). Of course this assumes that a reasonable number of rain gages are available under the radar umbrella to satisfactorily removing the mean bias. Also, assuming that the mean bias is removed, the error associated with the exponent is not excessive if a nominal value is chosen (e.g., 1.4) since errors caused by the Z-R relationship tend to cancel as data are averaged over greater space and time scales as shown in Figure 5-2 (Hudlow and Arsell 1978).

Physical mechanisms that can alter particle size distribution and, consequently, a Z-R relationship include: evaporation, accretion, coalescence, breakup, size sorting, and vertical and horizontal wind motion. Non-spherical ice particles and the flattening of raindrops as their size increases can enhance or reduce radar reflectivity measurements several decibels, depending on the radar polarization, and contribute errors to estimates of the precipitation rate. Mixed precipitation types, e.g., rain and hail in thunderstorms or rain and snow, can significantly alter a Z-R relationship. One means of minimizing the hail effect is to impose a maximum threshold on the precipitation rate (often ~ 53 dBZ). The threshold should be based on a maximum precipitation rate that can be expected in a given area. The presence of radar echoes beyond the threshold would then indicate the probability of hail and that specified upper limits of precipitation rate should not be exceeded.

Attempts have been made to determine Z-R variations based on other meteorological information such as storm type and various weather conditions; however, limited benefit was derived for reducing precipitation rate uncertainty (Stout and Mueller 1968).

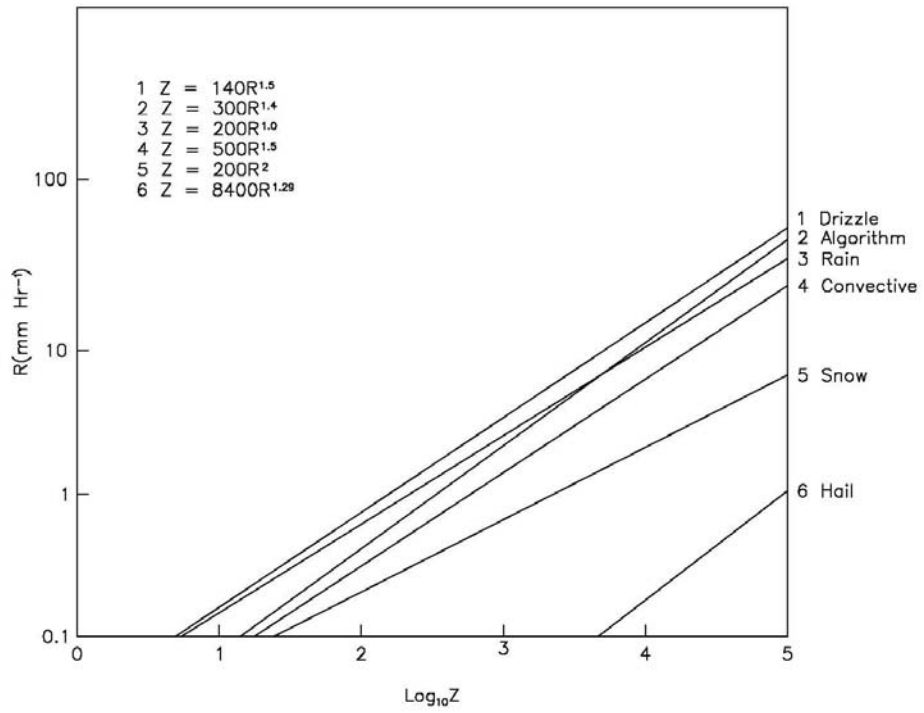


Figure 5-1
Plots of Z-R Relationships Illustrate the Variability of
Various Forms of Precipitation

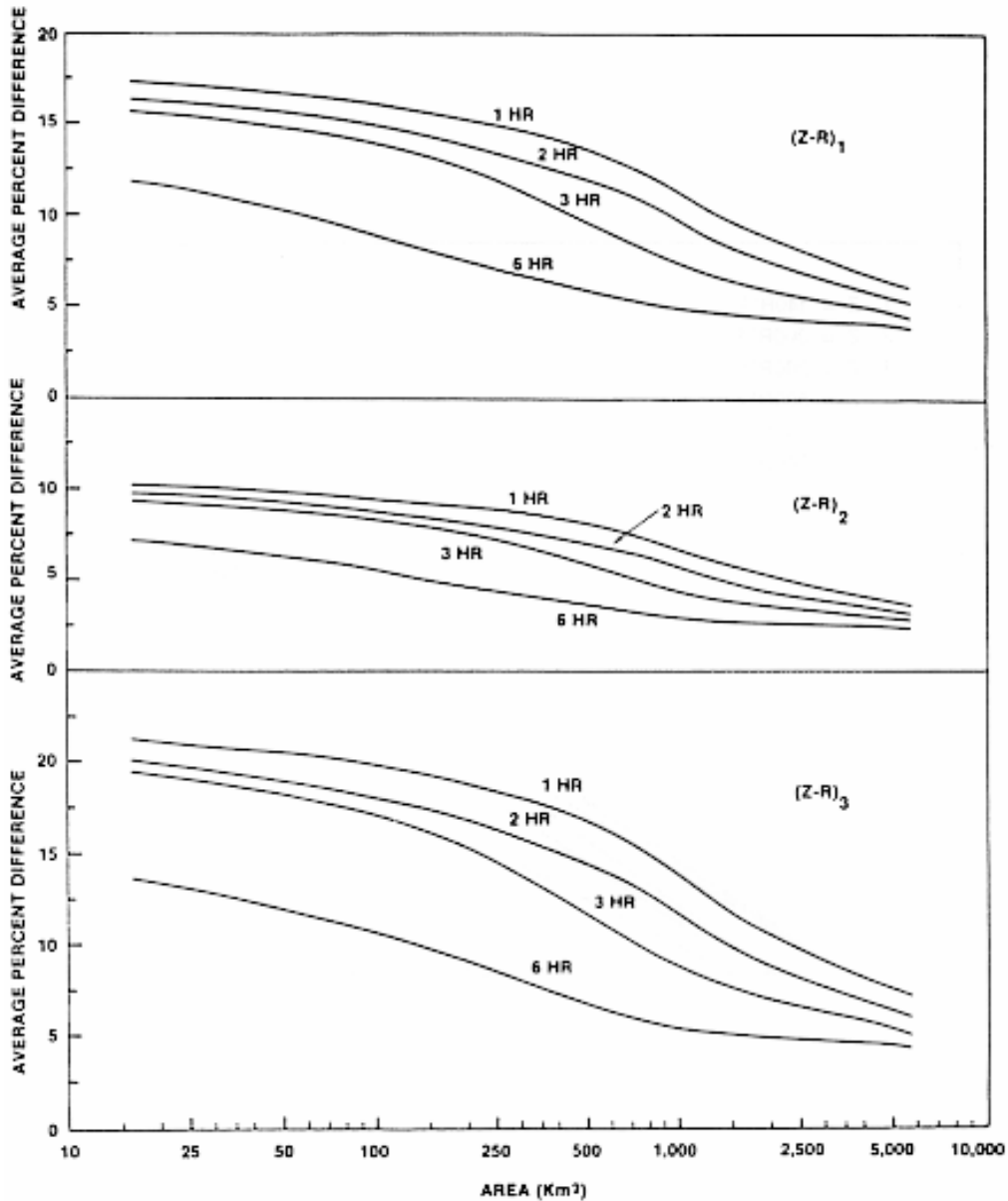


Figure 5-2
Mean Absolute Percent Difference Between Rainfall Estimates
Based on Z-R Relationships

Differences from a Z-R relationship of $Z = 230R^{1.25}$ and $(Z-R)_1$ of $Z = 170R^{1.52}$, $(Z-R)_2$ of $Z = 300R^{1.4}$, and $(Z-R)_3$ of $Z = 200R^{1.6}$, for a range of spatial averaging and temporal integration scales. Phase mean biases were removed before compilation of differences. This figure is based on the analysis of GARP Atlantic Tropical Experiment (GATE) data (Hudlow and Arkell 1978).

The previous discussion assumes that the precipitation estimates are based on radar pulses with a single polarization, usually horizontal. The introduction of dual-polarization capability promises to significantly increase the accuracy of precipitation identification and quantitative measurement (Ryzhkov and Zrnic 1996). In a dual-polarization system, the separate returned power estimates in both the horizontal and vertical sense can be used to infer the aspect ratio of the backscatterers. For example, small raindrops are nearly spherical, and yield nearly identical backscatter in both channels (Schaar et al. 2001). Larger raindrops tend to be more oblate due to viscous drag effects, and therefore yield significantly larger backscatter in the horizontal channel than in the vertical. The dual-polarization capability also greatly facilitates discrimination among different hydrometeor types, and between hydrometeors and other common targets such as birds, insect, and radar-cloaking chaff.

5.3.3 Time and Space Averaging. WSR-88D data are obtained by scanning in azimuth at a series of low elevation angles and making measurements at discrete range and angular intervals. The equivalent reflectivity factor values are converted to rainfall rate with an appropriate Z-R relationship and accumulated in time to yield a spatial distribution of precipitation depth.

Regardless of the Z-R relationship used, this procedure results in time and space sampling errors. Figure 5-3 illustrates the increase in these errors as the sampling interval is increased over the various averaging areas. For example, the top graph in Figure 5-3 shows for this data set that increasing the sampling interval from 5 to 10 minutes increases the hourly precipitation estimate error on the average of about 5 to 15 percent, depending on the averaging area. For a given sample interval, the percent differences decrease with increasing averaging area and integration time.

5.3.4 Below-Beam Effects. Below-beam effects result from the evaporation or growth of precipitation below the radar beam as well as horizontal motion of descending precipitation. At greater radar ranges with larger sampling volumes and with increasing beam height, the correlation between radar estimated and measured ground-level precipitation diminishes. An extreme example of below-beam effects is total evaporation of precipitating water. Thus, precipitation shown on the radar display at far ranges may not reach the ground at all. Comparison with rain gage observations and other surface synoptic data can offer help in identifying this problem. In many cases, access to other radars closer to the area of rainfall ambiguity is better at estimating accumulated rainfall than a distant radar.

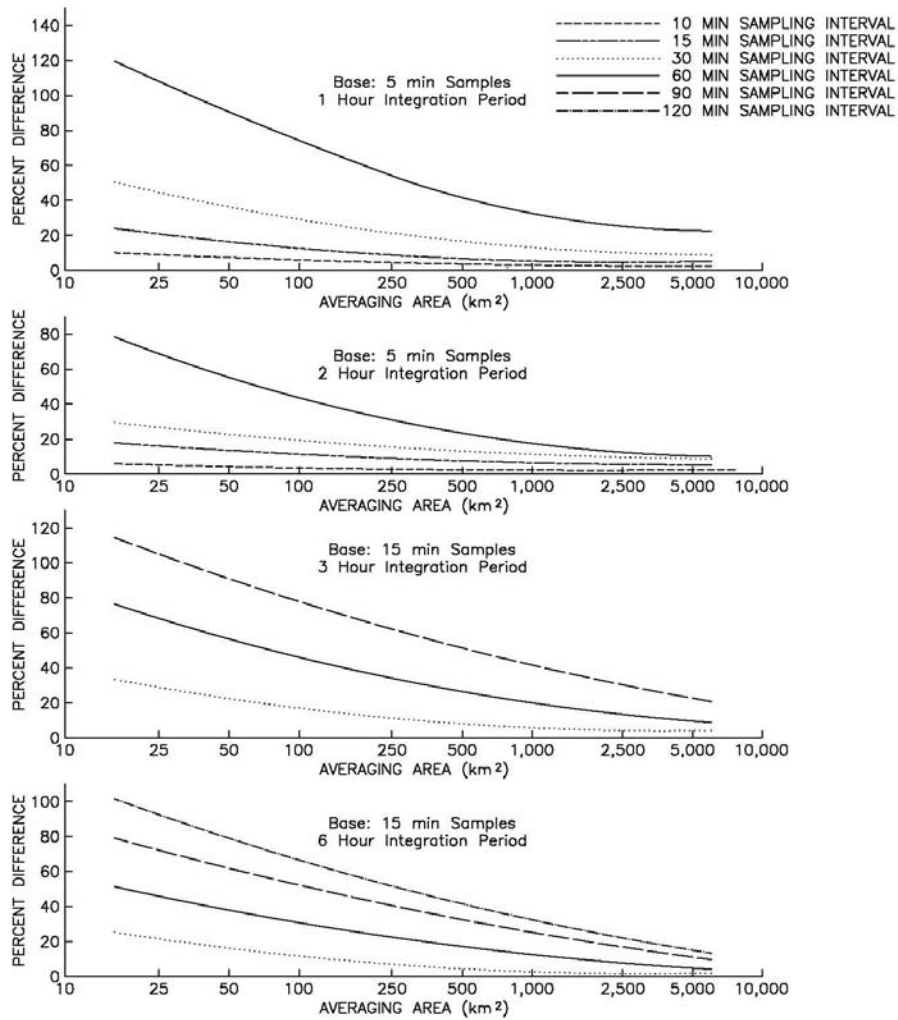


Figure 5-3
Mean Absolute Percent Difference Between Rainfall Estimates
Based on Sampling

Upper two panels: Using five-minute base sampling intervals and those from coarser sampling intervals for spatial averaging and temporal integration scales. Lower two panels: Same as upper two, except 15-minute base sampling interval was used and longer integration periods were included. This figure is based on the analysis of GARP Atlantic Tropical Experiment (GATE) data (Hudlow and Arkell 1978).

5.3.5 Effects of the Vertical Reflectivity Profile. In addition to near-surface evaporation or raindrop growth below the radar beam, precipitation systems generally feature a nonuniform reflectivity profile in the vertical. Most surface rainfall originally forms as snow above the freezing level. In stratiform rain situations, the radar detects dry snowflakes at longer ranges where the lowest beam is centered above the freezing level. Since ice hydrometeors return less radio power than liquid water, the estimated rainfall rate is significantly smaller than that observed at the surface. There is enhanced reflectivity due to melting, water-coated snowflakes in the layer just below the freezing level, and thus where the lowest beam intersects the melting layer the surface rain rate is overestimated (the bright-band effect). These effects become apparent with increasing radar range, and are often referred to collectively as range effects.

Correction for range effects is possible through the application of a climatic vertical profile, or through objective identification of the profile in real time, based on volumetric scanning. Both methods have achieved some success (Seo et al. 2000).

5.4 Adjustment of Radar-Derived Precipitation Estimates. Very large storm-to-storm and within storm errors in radar precipitation estimates can result from error sources described above. Errors of up to a factor of 2 are not uncommon; errors up to a factor of 5 or more sometimes occur (of course, as illustrated above, many factors affect the magnitude of the errors, especially the spatial and temporal scales over which the precipitation estimates are averaged). These errors can be reduced to various degrees by a number of adjustments and corrections to the radar-derived precipitation estimates. The simplest of these adjustments are applied to the radar parameter itself. More sophisticated procedures combine radar estimates with other hydrological and meteorological data. These adjustments are described in the following sections.

5.4.1 Adjustments Using Radar Parameters Alone. Many of the error sources discussed in Section 5.3 can be reduced by quality control and adjustment procedures operating on the radar data alone. Examples include the following:

- Oxygen absorption corrections
- Assignment of zero values to all reflectivities below a given noise threshold
- Ground clutter suppression procedures
- Corrections for beam blockage
- Isolated bin and other outlier checks
- Use of multiple elevation angles
- Adjustment of Z-R relationship for precipitation type and/or climatology and season

The precipitation estimation procedures of the WSR-88D employ many of these quality control and adjustment procedures (Part C, Chapter 3, of this Handbook).

5.4.2 Adjustment with Rain Gages. Techniques for adjusting radar precipitation estimates with rain gage observations take advantage of the superior ability of the radar to sample comprehensively the temporal and spatial precipitation distribution and the ability of the rain gages to measure relatively accurately the precipitation depth at the surface. Such adjustment, if carried out properly, will reduce errors in radar precipitation estimates caused by all the factors described previously, including those caused by an inadequate Z-R relationship (Anagnostou et al. 1998; Seo et al. 1999).

One must keep in mind that even if there were no actual errors in either gage or radar measurements, there are still discrepancies that result from differences in sampling mode (Anagnostou and Krajewski 1999). The radar beam and pulse volume samples instantaneously a large volume of atmosphere that may be several thousands of feet above ground and may have a surface projection of more than a square mile. The radar measurements are repeated at intervals of 4 to 10 minutes. The gage continuously records precipitation falling on an area that is smaller than a square foot. Precipitation intensity often varies significantly over distances of less than a mile and may change during time intervals of less than a minute. Therefore, the precipitation sampled by the gage may not be representative of that in the entire area beneath the radar-sampled volume. (Additionally, wind flow over rain gages and gage sampling techniques will also contribute to gage errors.) Similarly, rain rates observed instantaneously by the radar in any given measurement bin may not be representative of intensities during the intervals between observations (Austin 1987). These sampling-related discrepancies are very important to procedures that adjust radar estimates to match gage data. Techniques that force agreement at a few gage sites and extend the correction outward to adjacent measurement bins are especially sensitive to these discrepancies.

Intuitively, we expect the radar, even if only roughly calibrated, to measure the precipitation over the entire area observed by the radar to be better than a single gage. Conversely, if the network of calibrating gages were very dense under the entire radar umbrella, we would not expect the addition of radar to provide significant improvement (Wilson and Brandes 1979).

Procedures used to adjust radar precipitation estimates with rain gage data involve a variety of spatial adjustment techniques; some of the more notable will be discussed next.

5.4.2.1 Single-Parameter Rain Gage Data Adjustments. The simplest class of adjustments compares radar with rain gages to come up with a single "correction factor" that is then applied uniformly to the radar precipitation estimate. A common approach has been to compute the mean radar bias by averaging the sum of the Gage/Radar (G/R) ratios over some interval of time. Two major issues are whether the single correction factor is assumed to change with time and whether the procedure for estimating the correction factor is suitable for real-time applications (as opposed to post analysis). The adjustment procedure planned for eventual use in the WSR-88D

hydrologic software is in the class of time-varying, single-parameter rain gage data adjustments and is described in Part C, Chapter 3, of this Handbook.

5.4.2.2 Multi-parameter Rain Gage Data Adjustment. Various multiparameter procedures have been devised to combine radar observations routinely with distributed calibrating gages. With some procedures, local adjustments are made by computing G/R ratios at nearby calibration sites and then extrapolating the appropriate weights inversely by distance. In essence, the radar observations are molded to the gage observations by a plane-fitting technique while retaining the radar-indicated precipitation variability between gages. More sophisticated multivariate objective analysis approaches are also possible. A common multivariate objective analysis approach involves an optimal interpolation procedure that merges the radar and rain gage data in a multivariate analysis framework (Seo and Breidenbach 2002).

While multi-parameter rain gage data adjustments offer the promise of higher quality precipitation estimates, they are more computational demanding (sometimes much more) than single-parameter methods. They also tend to be more sensitive to the distribution in space and the accuracy of each gage data value used. For these reasons, the WSR-88D does not use multi-parameter rain gage data adjustments. However, such multivariate techniques have been implemented within the Advanced Weather Interactive Processing System (AWIPS), and have been used successfully as input to hydrologic models (Seo 1998).

5.4.3 Adjustments with Other Data. Clearly, the most accurate possible estimates of precipitation would optimally combine all available sources of information (e.g., radar, rain gage, satellite imagery, soundings, and surface data). Such a processing system would have to be extremely sophisticated, but the first steps in this direction will probably use satellite data along with radar and gage data. These types of procedures are considered to be outside the scope of the processing of the WSR-88D.

5.5 Concluding Remarks. As has been shown in the preceding discussion, there are many limitations in trying to correlate equivalent radar reflectivity factor with precipitation rate. Radar error patterns suggest that discrepancies occur from storm-to-storm in a systematic and perhaps predictable manner. The search for systematic error patterns and causes holds promise, but until this knowledge can be applied fully to radar measurements, the use of gage data to calibrate radar data is the most promising approach. Such approaches, however, must be applied with great care, and the adjustment procedure adopted must be formulated to ensure numerical stability and physically meaningful corrections.

The current operational WSR-88D processing system (Fulton et al. 1998) features many internal quality control measures and can be adapted to use several Z-R relationships. Radar-only precipitation estimates are likely to become substantially more accurate with the introduction of dual-polarization capabilities in the 2009 time frame.

REFERENCES

- Anagnostou, E. N., W. F. Krajewski, D.-J. Seo, Dong-Jun, and E. R. Johnson, 1998: Mean-field rainfall bias studies for WSR-88D. *J. of Hydrologic Engrg*, **3**, 149-159.
- Anagnostou, E. N., and W. F. Krajewski, 1999: Uncertainty quantification of mean-areal radar-rainfall estimates. *J. Atmos. Oceanic Technol.*, **16**, 206-215.
- Ahnert, P. R., M. D. Hudlow, E. R. Johnson, D. R. Greene, and M. Diaz, 1983: Proposed "on-site" precipitation processing system for NEXRAD, Preprints, *21st Conference on Meteorology*, Edmonton, Canada, Amer. Meteor. Soc., 378-385.
- Austin, Pauline M., 1987: Relation between Measured Radar Reflectivity and Surface Rainfall. *Mon. Wea. Rev.*, **115**, 1053-1070.
- Battan, L. J., 1973: *Radar Observations of the Atmosphere*. Univ. of Chicago Press, 323 pp.
- Cairns, M.A., Huggins, and S. Vasiloff, 1998: Precipitation algorithm improvements in the Eastern Sierra. NWS Western Region Technical Attachment, No. **98-08**, Salt Lake City, UT, 5 pp.
- Douglas, R. H., 1963: *Size distribution of Alberta hail samples*. Sci. Rept. MW-36. Montreal: Stormy Weather Group, McGill Univ., 71 pp.
- Hudlow, M., and R. Arkell. 1978: Effect of Temporal and Spatial Sampling Errors and Z-R Variability on Accuracy of GATE Radar Rainfall Estimates. Preprints, *18th Conference on Radar Meteorology*, Atlanta, GA, Amer. Meteor. Soc. 342-349.
- Hudlow, M. D., R. Arkell, V. Patterson, P. Pythowany, F. Richards, and S. Goetis, 1979: *Calibration and intercomparison of the GATE C-band radars*. NOAA Tech. Report EDIS 31, NTIS, Springfield, VA.
- Huggins, A. and D. Kingsmill, 1998: Improvements of WSR-88D algorithms in the intermountain west with applications to flash flood forecasts and wintertime QPFs. CIASTA Annual Report on Progress under Task II: Weather Research, Desert Research Institute, Dandini Research Park, Reno, NV, 26 pp.
- Joss, J. K., K. Schram, J. D. Thams, and A. Waldvogel, 1970: *On the quantitative determination of precipitation by radar*. Wissenschaftliche Mitteilungen Nr. 63, Eidgenossischen Kommission Zum Studium der Hagelbildung und der Hagelabwehr, 38 pp.
- Marshall, J. S., and W. M. Palmer, 1948: The distribution of raindrops with size. *J. Appl. Meteor.*, **5**, 165-166.

- Martner, B. E., 1977: A field experiment on the calibration of radars with raindrop disdrometers. *Appl. Meteor.*, **16**, 451-454.
- Quinlan, J.S. and E.J. Sinsabaugh, 1999: An evaluation of the performance of the snow algorithm at NWFO Albany, NY during the 1997-98 winter season. Preprints, *29th Int. Conf. on Radar Meteorology.*, Montreal, Quebec, CA, Amer. Meteor. Soc., 794-979.
- Schuur, T. J., A. V. Ryzhkov, D. S. Zrnić, and M. Schönhuber, 2001: Drop size distributions measured by a 2D video disdrometer: Comparison with dual-polarization radar Data. *J. App Meteor.*, **40**, 1019-1034.
- Seo, D. J., J. P. Breidenbach, and E. R. Johnson, 1999: Real-time estimation of mean field bias in radar rainfall data. *J. Hydrology*, **223**, 131-147.
- Seo, D. J., 1998: Real-time estimation of rainfall fields using radar rainfall and rain gage data. *J. Hydrology*, **208**, 37-52.
- Seo, D. J., J. Breidenbach, R. Fulton, and D. Miller, 2000: Real-time adjustment of range-dependent biases in WSR-88D rainfall estimates due to nonuniform vertical profile of reflectivity. *J. Hydrometeorology*, **1**, 222-240.
- Seo, D. J., and J. P. Breidenbach, 2002: Real-Time Correction of Spatially Nonuniform Bias in Radar Rainfall Data Using Rain Gauge Measurements. *J. Hydrometeorology*, **3**, 93-111.
- Stout, G. E., and E. A. Mueller, 1968: Survey of relationships between rainfall rate and radar reflectivity in the measurements of precipitation. *J. Appl. Meteor.*, **7**, 465-474.
- Wilson, J. W., 1975: *Radar-gage precipitation measurements during the IFYGL*. The Center for the Environment & Man, Inc., Report 4177-540.
- Wilson, J. W., and E. A. Brandes 1979: Radar measurement of rainfall--a summary. *Bull. Amer. Meteor. Soc.*, **60**, 1048-1058.